© 2019. Published by The Company of Biologists Ltd | Journal of Cell Science (2019) 132, jcs226076. doi:10.1242/jcs.226076

RESEARCH ARTICLE

Shear stress-induced nuclear shrinkage through activation of Piezo1 channels in epithelial cells

Deekshitha Jetta[1], Philip A. Gottlieb[2], Deepika Verma[1], Frederick Sachs[2] and Susan Z. Hua[1,2,*]

ABSTRACT

The cell nucleus responds to mechanical cues with changes in size, morphology and motility. Previous work has shown that external forces couple to nuclei through the cytoskeleton network, but we show here that changes in nuclear shape can be driven solely by calcium levels. Fluid shear stress applied to MDCK cells caused the nuclei to shrink through a Ca^{2+}-dependent signaling pathway. Inhibiting mechanosensitive Piezo1 channels through treatment with GsMTx4 prevented nuclear shrinkage. Piezo1 knockdown also significantly reduced the nuclear shrinkage. Activation of Piezo1 with the agonist Yoda1 caused similar nucleus shrinkage in cells not exposed to shear stress. These results demonstrate that the Piezo1 channel is a key element for transmitting shear force input to nuclei. To ascertain the relative contribution of Ca^{2+} to cytoskeleton perturbation, we examined F-actin reorganization under shear stress and static conditions, and showed that reorganization of the cytoskeleton is not necessary for nuclear shrinkage. These results emphasize the role of the mechanosensitive channels as primary transducers in force transmission to the nucleus.

KEY WORDS: Ca^{2+} signaling, Mechanosensitive channel (MSC), Mechanosensors, Piezo1 channels, MDCK cells

INTRODUCTION

The cell nucleus undergoes changes in size, shape and motility under the influence of local mechanical perturbations (Ihalainen et al., 2015; Wang et al., 2009). This dynamic process also allows cells to regulate gene expression (Aarts et al., 2002; Gupta et al., 2012; Philip and Dahl, 2008), DNA structure, and chromosome segregation (Arnone et al., 2013; Arsenovic et al., 2016). Abnormal nuclear changes give rise to a variety of diseases (Hale et al., 2008; Isermann and Lammerding, 2013; Lammerding et al., 2005). The shape of a nucleus is defined by the nuclear envelope consisting of scaffold lamina (Broers et al., 2006; Stuurman et al., 1998) that connects to the surrounding cytoskeleton via the linker of nucleoskeleton and cytoskeleton (LINC) complex (Chang et al., 2015; Crisp, 2006; Ihalainen et al., 2015; Lombardi et al., 2011; Versaevel et al., 2014). External forces that change the cell's mechanical environment around the nucleus can be directly monitored by cytoskeleton distortion (Li et al., 2014b). Using patterned substrates, it has been shown that mechanically confining a cell shape caused the nuclear envelope to undergo significant deformation (Bray et al., 2010; Grevesse et al., 2013; Versaevel et al., 2012). Substrate rigidity also affects nuclear shape. Cells grown on hard substrates have thin spreading nuclei, while cells on soft substrates developed thicker nuclei with smaller spreading areas (Ihalainen et al., 2015; Lovett et al., 2013). However, under low shear stress, an actin cap forms and connects to the nucleus (Chambliss et al., 2013), suggesting that more sensitive force sensors may be required to transmit shear forces to the nucleus.

Recently, mechanosensitive Piezo channels (Piezo1 and Piezo2) have emerged as sensors of mechanical stimuli (Coste et al., 2010, 2012). Piezo proteins are the subunits of Ca^{2+}-permeable non-selective cation channels that respond to mechanical forces (Coste et al., 2010, 2012). The Piezo1 protein is expressed in all organs including the kidney (Coste et al., 2010), and is involved in integrin activation (McHugh et al., 2010). Piezo1 also acts as a flow sensor in endothelial cells involved in vascular development (Chang et al., 2015; Li et al., 2014a; Ranade et al., 2014). Recent studies have shown that Piezo1 is required for mechanically regulated stem cell differentiation through Ca^{2+} signaling (He et al., 2018) and that neural stem cells require Ca^{2+} influx through Piezo1 for the decision to differentiate into neurons or astrocytes (Pathak et al., 2014).

Intracellular Ca^{2+} elevation in response to mechanical stimuli is universal. Free Ca^{2+} in a cell can increase rapidly upon the stimulation, well before the reorganization of cytoskeleton and nuclear deformation (Verma et al., 2012) and Ca^{2+} is an important second messenger responsible for many physiological processes including myosin-driven contractility (Karaki et al., 1997). A key linker protein in the LINC complex, Nesprin-2G (also known as Syne2), responds to myosin-dependent contractile forces in adherent cells, leading to changes in nuclear morphology and translocation (Arsenovic et al., 2016). Elevated free Ca^{2+} concentration causes chromatin condensation in nuclei (Chan et al., 2017). Thus, Piezo-mediated Ca^{2+} signaling may contribute to force transduction, in parallel with direct mechanical interactions of actin with the nuclear lamina.

Here, we show that the Piezo channels are able to modulate nuclear size in MDCK cells under fluid shear stress. This effect is inhibited by the channel gating inhibitor, GsMTx4, and by Piezo1 silencing using miRNA. To distinguish between Ca^{2+} signaling and shear-induced cytoskeleton reorganization, we activated Piezo1 with the agonist Yoda1 in the absence of shear stress. Our results show that Piezo1-mediated Ca^{2+} elevation is adequate for shear stress-induced nuclear changes and actin reorganization.

RESULTS

Fluid shear stress causes nuclear shrinkage in epithelial cells

We measured changes in the nucleus spreading area of MDCK cells subjected to fluid shear stress (1.1 dyn/cm^2) in the microfluidic channel, and found that shear stress caused a reduction of nuclear area with a maximum reduction of ~50% (Fig. 1A,B; also see Movie 1). Multiple experiments showed that the shear-induced nuclear shrinkage

[1]Department of Mechanical and Aerospace Engineering, University at Buffalo, Buffalo, NY 14260, USA. [2]Department of Physiology and Biophysics, University at Buffalo, Buffalo, NY 14260, USA.

*Author for correspondence (zhua@buffalo.edu)

S.Z.H., 0000-0002-4410-697X

Received 1 October 2018; Accepted 29 April 2019

Journal of Cell Science (2019) 132, jcs226076. doi:10.1242/jcs.226076

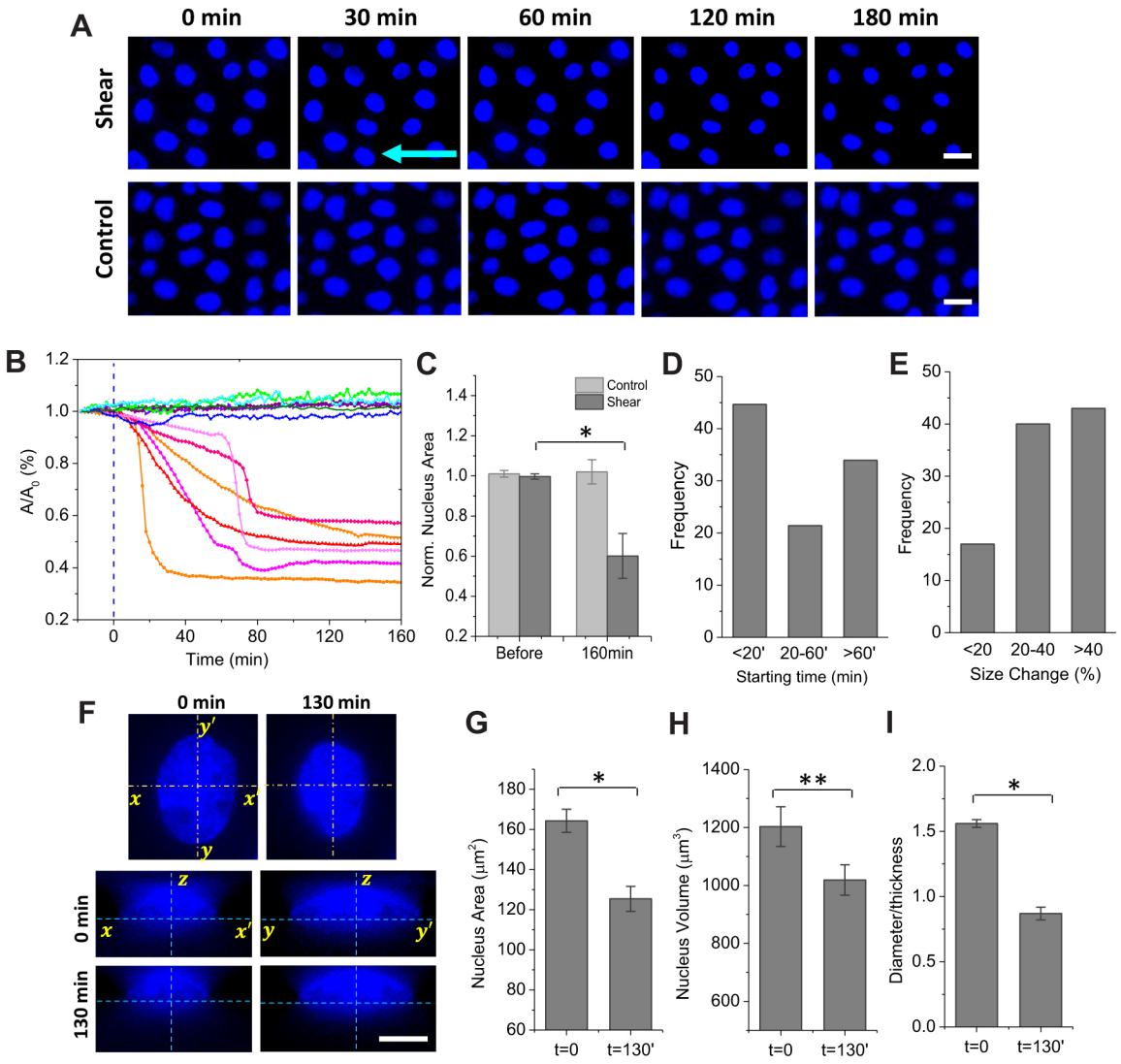

Fig. 1. Effect of shear stress on nucleus spreading area. (A) Fluorescent images of nuclei of MDCK cells subjected to shear stress (1.1 dyn/cm^2, upper panel) and under static conditions (lower panel), showing that the spreading area of the nucleus decreased with flow. Nuclei visualized with Hoechst 33342 dye. The arrow indicates flow direction. Scale bars: 20 µm. (B) Changes of nuclear area in cells subject to shear stress (warm colors) and control cells (cool colors), showing that nuclei shrinkage occurred between 10 and 80 min after shear flow was initiated (blue dashed line). (C) Maximum area changes before and 160 min after flow or in static condition (n=50, *P<0.001). (D,E) Histograms of shrinkage starting times (D) and area changes (E) under flow (n=50 for each). (F) Z-stack images of a nucleus in plane-view (upper panels) and cross-section of xz and yz planes (lower panels), before and after shear stress, showing the nucleus shrunk after being subjected to shear stress. Scale bar: 10 µm. (G–I) Area (G), volume (H), and diameter to thickness ratio of the same nuclei under shear stress (n=20, *P<0.001, **P<0.005 by paired-sample t-test). This confirms that the measured reduction in nuclear area represents the nuclear shrinkage. Error bars indicate s.e.m.

was consistent (Fig. 1C, n=50). The onset of shrinkage varied from 10 to 60 min, often showing a profound latency (Fig. 1D). Most cells reached a minimal nuclear area within ∼80 min (Fig. 1A,D). The size reduction occurred in 80% of cells. The other 20% had insignificant changes within the experimental period of 2.5 h (Fig. 1E).

To verify that changes in nuclear area represent a change in volume, we recorded z-stack images and measured the changes in three dimensions (x, y, z) before and after shear stress of the same cells. The planar area in each member of the stack was reduced significantly after 2 h of shear (x and y; Fig. 1F,G), while the thickness of the nucleus (z) increased, but to a lesser extent (Fig. 1F). This resulted in a reduction in nuclear volume. The changes in nuclear volume were statistically significant (Fig. 1H; n=20, P<0.005). Confocal microscopy of fixed cells with immunostaining for lamin-A and phalloidin showed that the ratio of nuclear diameter to height (thickness) was ∼25% lower in cells subjected to shear stress (Fig. S1C; n=50, P<0.001), consistent with live cell measurements on the same cells (Fig. 1I; n=20, P<0.001). Confocal images of Hoechst-stained nuclei showed that chromatin is evenly distributed in resting nuclei without flow, but condensed at the nuclear periphery and around nucleoli after shear flow (Fig. S1D). A similar effect appears with Yoda1-elicited nuclear shrinkage without flow (see later sections). Taken together, these results suggest that nuclear shrinkage relates to chromatin condensation.

To assess the effect of shear stress on viability, propidium iodide was loaded at the end of flow experiments. More than 90% of cells were deemed viable after 2.5 h of shear stress (Fig. S2), consistent with our previous report that under the same fluid shear stress the reorganization of cytoskeleton in MDCK cells was reversible (Verma et al., 2012).

Journal of Cell Science (2019) 132, jcs226076. doi:10.1242/jcs.226076

Inhibiting Piezo1 channels eliminates nucleus shrinkage

Piezo proteins function as Ca^{2+}-permeable cation channels that are opened in response to shear stress in endothelial cells (Li et al., 2014a). To investigate whether Piezo1 is responsible for the nuclear response in MDCK cells, we inhibited Piezo1 with the specific inhibitor GsMTx4 (Bae et al., 2011), which led to a reduction in nuclear shrinkage under flow (Fig. 2A, blue curve). Treatment with GsMTx4 also inhibited the shear-induced Ca^{2+} elevation (Fig. 2B, blue curve). As controls, we tested the non-specific channel inhibitor Gd^{3+} that inhibits most mechanosensitive channels (MSCs), including Piezo1. It too inhibited Ca^{2+} influx and eliminated nuclear shrinkage (Fig. 2A,B, dark green curves). As a second control, we used a Ca^{2+}-free saline bath and obtained consistent results (Fig. 2A, green curve). The effect of Piezo1 inhibition on changes of nucleus sizes is statistically significant (Fig. 2C; n=50, P<0.001 for all conditions), indicating that Piezo1 plays a role in the response to shear stress in MDCK cells, and likely functions through Ca^{2+} signaling.

Piezo1 is required for shear-induced nuclear changes

To verify if Piezo1 is necessary for shear stress transduction, we targeted *Piezo1* with miRNA and measured the nucleus response to shear stress after knockdown. Cells were transfected with *Piezo1* miRNA and co-expressed with EGFP to verify transfection (Fig. 3A). Knockdown efficiency was assessed using immunostaining for Piezo1, and quantitative RT-PCR (Fig. S3A–D). Knockdown of Piezo1 reduced the Ca^{2+} rise under shear stress (Fig. 3B, blue curves). The peak Ca^{2+} in transfected cells was ∼90% lower than non-transfected cells within the same region of the slide (Fig. 3B, red curves). The response of cells transfected with non-targeting RNAi (mock-transfected) was similar to the control cells (Fig. 3B, gray curves). As expected, the change in nuclear area was reduced to <10% in *Piezo1* knockdown (P1KD) cells (Fig. 3D, blue curves). In contrast, the mock-transfected and non-transfected cells showed >25% reduction in nuclear area (Fig. 3D, gray and red curves). These results are consistent in >10 experiments and the difference between the responses in P1KD versus control cells was statistically significant (Fig. 3C,E; n=60, P<0.001, for all conditions). *Z*-stack images of P1KD cells before and after shear stress showed a minimal change in volume and diameter to height (thickness) ratio (Fig. S3E–G; n=20). For some P1KD cells, we observed small changes in Ca^{2+} influx, and for other cells, the nucleus area shrinkage occurred after 2 h of flow. We presume that these responses are due to the existence of other mechanosensitive cation channels in MDCK cells or that the knockdown efficiency of *Piezo1* is not 100%. These results support the hypothesis that Piezo1 channels are utilized in the nuclear response to shear and that they function through Ca^{2+} signaling.

Piezo1 regulates nuclear response to shear forces via Ca^{2+} signaling

To decouple Piezo1-mediated Ca^{2+} signaling from the cytoskeleton reorganization that occurs under shear stress, we activated Piezo1 channels with the agonist Yoda1 (Syeda et al., 2015) with no flow. Yoda1 (25 µM) evoked a Ca^{2+} influx, resulting in nuclear shrinkage to 25% of the resting area (Fig. 4A,C, red curves), similar to the response seen under shear stress. The effect was eliminated in a Ca^{2+}-free solution (Fig. 4A,C, gray curves). If Ca^{2+} is the key messenger modifying nuclear shape, the Ca^{2+} rise resulting from other stimuli should also change nuclear size. To test this, we elicited a Ca^{2+} rise by applying multiple agents to the cells. Cells showed a similar nuclear size change when treated with thapsigargin (Tg, 5 µM), which causes Ca^{2+} release from ER stores (Fig. 4A,C, pink curves). The Ca^{2+} carrier ionophore A23187 (2 µM) produced a similar change in nuclear dimensions (Fig. 4A, orange curve). The effects of Ca^{2+} manipulation on nuclear changes were statistically significant (Fig. 4B,D), and appeared independent of the Ca^{2+} source. Note that as Tg caused a lesser Ca^{2+} rise than Yoda1 but a greater nuclear reduction, it is possible that Tg also affects other Ca^{2+}-sensitive processes.

Next, we examined the cytoskeleton reorganization elicited by Yoda1 and the other treatment agents and found that actin bundles persisted in the cells despite the Ca^{2+} rise (Fig. 4E). This is in sharp contrast with shear stimulation, where the cytoskeleton massively

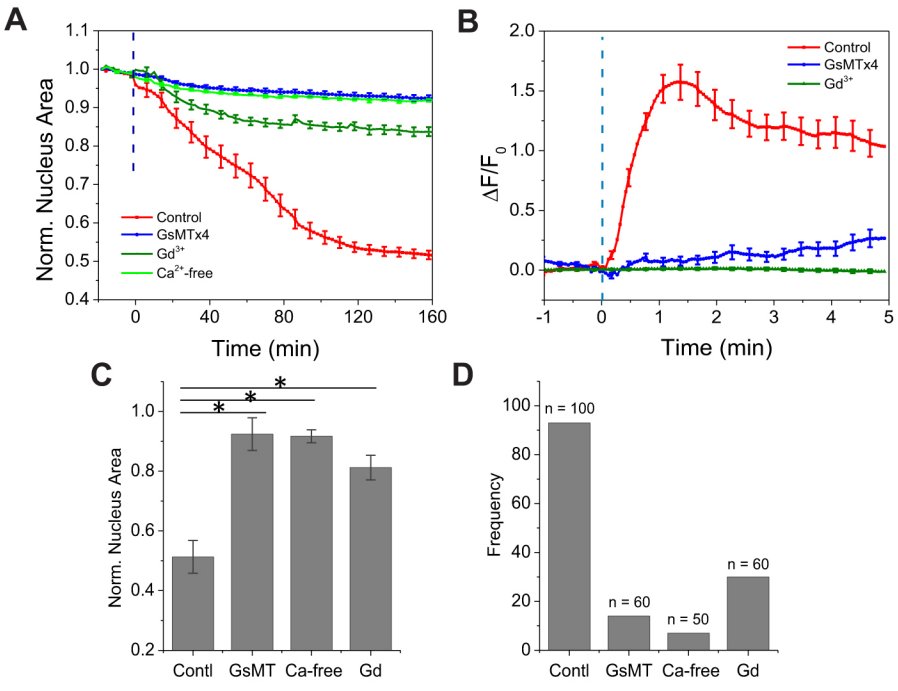

Fig. 2. Effect of Piezo1 inhibitors on nuclear response to shear stress. (A) Changes of nucleus area in response to shear stress (1.1 dyn/cm^2) were eliminated in the presence of GsMTx4 (5 µM), Gd^{3+} (20 µM), and in Ca^{2+}-free solution, showing that inhibition of Piezo1 channels inhibited nuclear shrinkage under flow (n=50 for each curve, area normalized to the area at time zero). (B) Inhibition of the Ca^{2+} response to shear stress applied to MDCK cells in the presence or absence of inhibitors. The change in Ca^{2+} intensity (ΔF) is normalized to intensity at time zero (F_0) (n=50 for each curve). Blue dashed line indicates initiation of shear flow. (C) Maximum nuclear changes in the presence of inhibitors and Ca^{2+}-free solution were compared with control cells under shear stress, showing the change in nuclear size is Ca^{2+} dependent (n=50 for each, *P<0.001 by two-sample t-test). (D) Histogram of number of responding nuclei (with shrinkage >10%) under flow in the presence of each inhibitor. Error bars indicate s.e.m.

Journal of Cell Science

Journal of Cell Science (2019) 132, jcs226076. doi:10.1242/jcs.226076

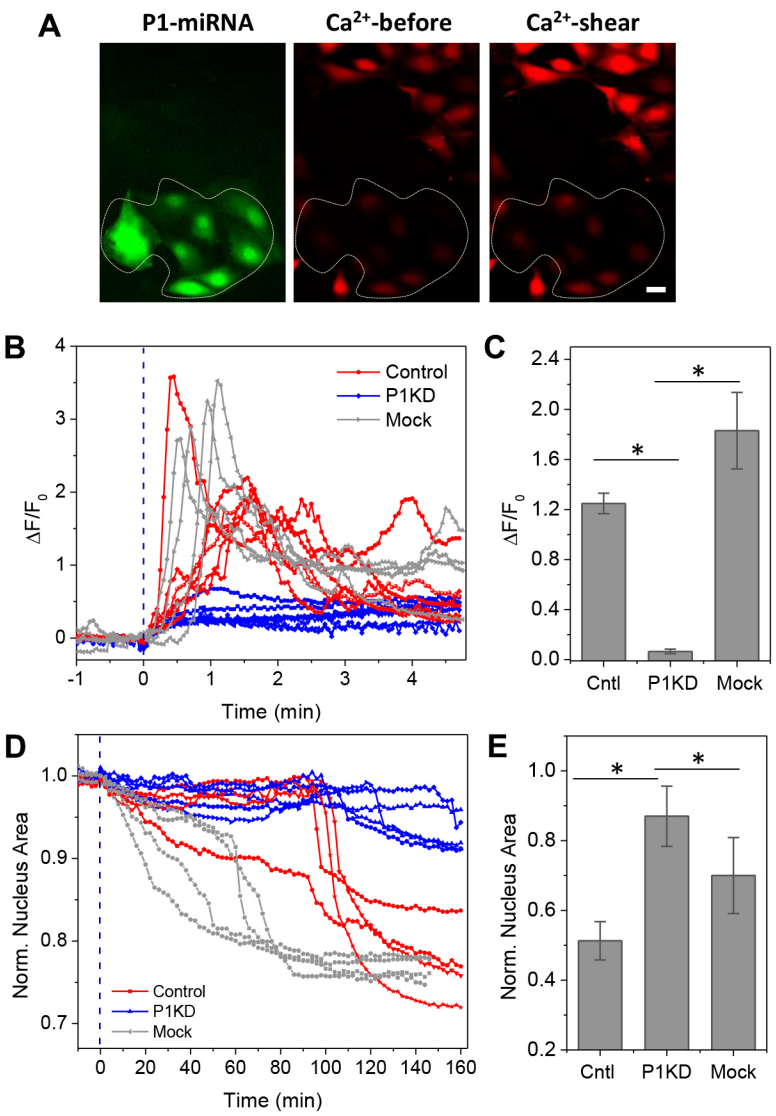

Fig. 3. Shear-induced Ca^{2+} influx and nuclear deformation are eliminated in Piezo1 knockdown (P1KD) cells. (A) Images of MDCK cells expressing miRNA that targets *Piezo1* (green, circled by dashed line) showed that they did not respond to shear stress. Cells that were untransfected had a robust Ca^{2+} (red) response to a shear stimulus (1.1 dyn/cm^2). Scale bar: 20 µm. (B) Time course of Ca^{2+} response in Piezo1 knockdown (P1KD) cells (blue curves), mock-transfected cells (gray curves), and control cells (red curves) following initiation of shear stress (blue dashed line), showing that Piezo1 is required for Ca^{2+} response. (C) Comparison of peak Ca^{2+} in P1KD cells with control cells (n=60, *P<0.001), and with mock-transfected cells (n=30, *P<0.001 by two-sample t-test) from multiple experiments. (D) Normalized nuclear areas in P1KD cells (blue curves), mock-transfected (gray curves) and control (red curves) cells, showing that shear stress induced minimal nucleus changes in P1KD cells. (E) Nuclear areas measured at 150 min from >10 experiments for each cell type (n=60, *P<0.001 by two-sample t-test). Error bars indicate s.e.m.

reorganized to form the actin ring along the cell periphery (Fig. 4F, shear control panel). Under shear stress, blocking Ca^{2+} influx with GsMTx4 or using a Ca^{2+}-free solution, inhibited cytoskeleton reorganization (Fig. 4F). This indicates that Piezo1-activated Ca^{2+} signaling is responsible for the nuclear shrinkage, and also contributes to cytoskeletal reorganization.

To further assess the role of the cytoskeleton in nuclear shrinkage, we treated the cells with cytochalasin-D, which inhibits actin polymerization. Disrupting actin filaments with cytochalasin-D (5 µM) caused a slow but significant reduction in nuclear size, and interestingly, intracellular Ca^{2+} levels increased (Fig. S4A–D). Immunostaining showed that stress fibers on the basement surface completely disassembled with cytochalasin-D treatment (Fig. S4E). This result supports the role of Ca^{2+} increase as the major factor for nuclear shrinkage.

DISCUSSION

It has been widely observed that local mechanical stimulation alters the shape and size of nuclei (Gupta et al., 2012; Ihalainen et al., 2015; Philip and Dahl, 2008; Zhu et al., 2016). Previous studies have emphasized the role of cytoskeletal distortion, with external forces transmitting the mechanical stress directly to the nuclear envelope (Balikov et al., 2017; Gupta et al., 2012; Li et al., 2014b; Lu et al., 2012). However, changes to the nucleus can occur even with very small stimuli (Chambliss et al., 2013), suggesting that the sensor need not be the cytoskeleton itself. In this work, we show that nuclear deformation under shear stress is Ca^{2+}-dependent, as supplied by Piezo1. The Ca^{2+} signaling causes nuclear deformations via a force transduction pathway independent of cytoskeletal reorganization.

Calcium signaling through Piezo1 is involved in a number of physiological responses. Stem cell differentiation in the *Drosophila* midgut (He et al., 2018) and neural differentiation to neurons and astrocytes (Pathak et al., 2014) are linked to Ca^{2+} influx through Piezo1. We recently showed that enhanced cell migration is linked to Ca^{2+} influx in cells overexpressing Piezo1 channels (Maneshi et al., 2018). This work extends these effects to morphological changes to the nucleus.

In culture, MDCK cells at rest have abundant thick stress fibers underneath the nucleus (Fig. S1A). We and others have studied cytoskeleton reorganization in MDCK cells under a variety of flow rates, and found that significant remodeling occurred at shear stresses of ∼1.0 dyn/cm^2 (Essig et al., 2001; Duan et al., 2008; Verma et al., 2012). Partial reorganization could occur at lower flow rate (Verma et al., 2012), and the shear stress threshold for Ca^{2+} is even lower. We have previously determined the threshold for Ca^{2+}

Journal of Cell Science (2019) 132, jcs226076. doi:10.1242/jcs.226076

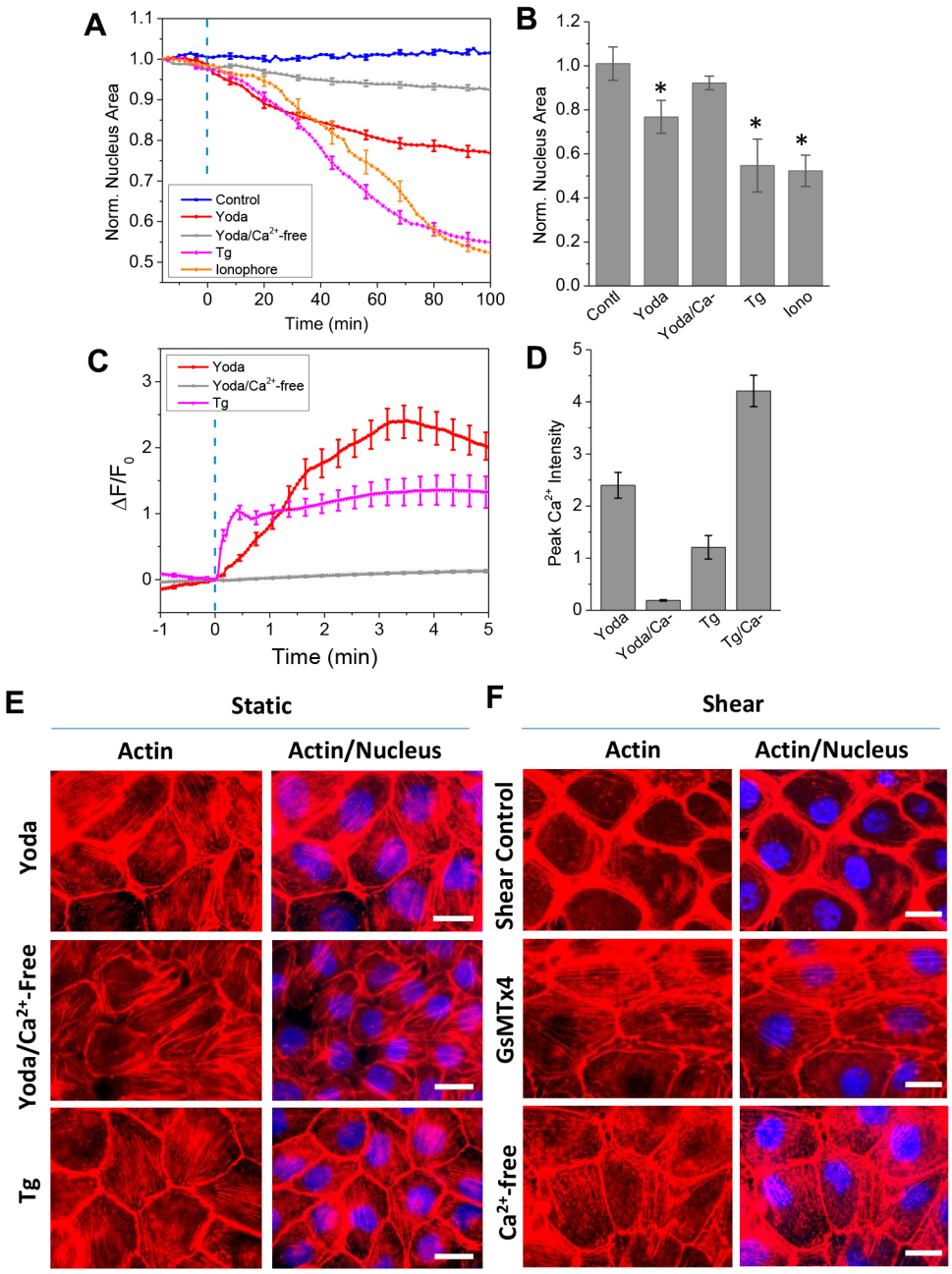

Fig. 4. Effect of agonist- or chemical-elicited Ca^{2+} rise on nuclear deformation. (A) Changes of nuclear area in response to Piezo1 agonist Yoda1 (25 µM), Tg (5 µM), ionophore A23187, and Yoda1 in Ca^{2+}-free solution, showing that similar nucleus shrinkage was observed after initiation of shear flow (blue dashed line) (n=30, for each condition). (B) Maximum area changes evoked by treatment with drugs are compared with control cells (n=30 for each condition, *P<0.001 by two-sample t-test). (C) Ca^{2+} responses to agonist or drugs, showing that a Ca^{2+} rise is accountable for nucleus shrinkage (n=30 for each condition). (D) Peak Ca^{2+} response to each compound (n=30 for each). (E) Images of actin (red) and lamin-A (blue) in cells exposed to 25 µM Yoda1 and 5 µM Tg in saline and Yoda1 in Ca^{2+}-free solutions without shear stress, showing that the drugs did not cause reorganization, but induced nuclear shrinkage. (F) Images of actin (red) and lamin-A (blue) in cells after 160 min shear flow in saline, 5 µM GsMTx4, or Ca^{2+}-free solutions, showing inhibition of Ca^{2+} influx eliminated reorganization. Scale bars: 20 µm. Error bars represent s.e.m.

response in our chamber is ∼0.07 dyn/cm^2 (Rahimzadeh, 2011). This suggests that epithelial cells have ultrasensitive sensors that can detect low shear stress. Nuclear deformation can occur at low shear stress when Ca^{2+} influx is triggered, and flow rate variation may contribute to the dynamic changes of nuclei.

Piezo1 has been found on the apical surface of MDCK cells, and Piezo1 channels can be activated to transport Ca^{2+} by changes in membrane tension (Gudipaty et al., 2017). In endothelial cells, Piezo1 is responsible for detecting blood flow in the vascular system, enabling endothelial cell alignment under shear stress (Li et al., 2014a; Ranade et al., 2014). In epithelial cells, membrane stretch activates Piezo1 channels that regulate cell division and extrusion through Ca^{2+} signaling (Eisenhoffer et al., 2012; Gudipaty et al., 2017). We previously reported that shear stress induces a Ca^{2+} influx in epithelial cells through Piezo-type mechanosensitive channels (Hua et al., 2010). By inhibiting Piezo1 during shear stress stimulation, we have now confirmed that nuclear deformation requires Ca^{2+} (Fig. 2). Conversely, by activating Piezo1 with the agonist, Yoda1, we induced similar nuclear changes in the absence of shear flow (Fig. 4). The nuclear dimensional changes occur independently of cytoskeletal perturbations by shear stress.

How does Ca^{2+} signaling activate the downstream events leading to nuclear deformation? One possibility is that Ca^{2+} concentration affects the permeability of nuclear pores to ions and small molecules, altering nuclear volume (Chan et al., 2017; Finan and Guilak, 2010). Isolated nuclei respond to an increase in ionic strength of the surrounding solution, such as Ca^{2+} concentration, with a drastic decrease in volume (Chan et al., 2017). These nuclei displayed condensed perinuclear chromatin and an uneven nuclear membrane (Chan et al., 2017). Our results show the same chromatin accumulation at the nuclear periphery after exposure to shear flow or

treatment with Yoda1 (Fig. S1D), suggesting that Ca^{2+}-dependent chromatin hypercondensation is the primary cause of substantial nuclear shrinkage. Additionally, Ca^{2+}-dependent myosin contractility could participate. Piezo-mediated Ca^{2+} rise activates myosin–Rho pathways in MDCK cells, which alters their contractility (Nourse and Pathak, 2017), resulting in the extrusions of crowded live cells (Eisenhoffer et al., 2012). We previously showed that a brief increase in contractile force triggered a subsequent reduction in cytoskeletal tension and reorganization under shear stress (Verma et al., 2012). Thus, Piezo-mediated Ca^{2+} signaling may activate myosin contractility (Eddy et al., 2000). Piezo1 may also work in concert with other signaling proteins, such as FAK (also known as PTK2) and Akt, that affect nuclear morphology (Uzer et al., 2015), or it may directly interact with Nesprin proteins and the lamina at the LINC complex (Arsenovic et al., 2016; Neelam et al., 2016). This is consistent with Piezo proteins being located at different subcellular sites including the plasma membrane, the nuclear envelope (Gudipaty et al., 2017) and the ER (McHugh et al., 2010). Further studies will need to examine the breadth of downstream signaling triggered by Piezo1 activation.

In conclusion, our studies demonstrate that Piezo1-mediated Ca^{2+} signaling is responsible for nuclear deformation under fluid shear stress. These results suggest a signaling pathway used by epithelial cells for transmitting mechanical force through the cell to alter nuclear shape and volume.

MATERIALS AND METHODS

Fluid shear stress experiments

Microfluidic chips with 1100 µm wide, 90 µm high and 15 mm long PDMS channels were fabricated using standard soft lithography (Pennell et al., 2008). The chips have a coverslip base coated with fibronectin (Sigma-Aldrich). During experiments, a chip was placed in a stage-top incubator (INUB-ZILCSD-F1-LU, Tokai Hit Co., Ltd) and maintained at 37°C and 5% CO_2. A syringe pump (Harvard Apparatus, PHD2000) perfused solution through the channel, applying fluid shear stress. The fluid shear stress (τ) was calculated using $\tau=6\,\mu Q/wh^2$, where $\mu=0.8\times10^{-3}$ Pa·s is the dynamic viscosity of the solution, Q is the volume flow rate, and w and h are the width and the height of the channel, respectively. The typical shear stress of 1.1 dyn/cm^2 matches physiological levels of urine flow (Zhou, 2009) and was used for all experiments.

Nuclear size measurements

The cell-permeable DNA stain, Hoechst 33342 dye (Thermo Scientific) was used to visualize nuclear geometry. The dye (1.6 µM) was loaded in the microfluidic channels and incubated for 10 min. Nuclear sizes were analyzed using the open-source image analysis software, CellProfiler (Carpenter et al., 2006), that measures and tracks the pixel area of each nucleus with time. The nuclear area was normalized to the area at time zero to assess relative changes.

Ca^{2+} and viability assays

Cytosolic Ca^{2+} was measured using two Ca^{2+}-sensitive dyes, Fluo-4 AM (5 µM, Invitrogen) for control cells and Calbryte 630 AM (20 µM, AATBIO) for Piezo1 knockdown (P1KD) cells. The dye was loaded into the cells either in the fluid channel or in a Petri dish, and incubated for 30 min at 37°C. The cells were then washed with isotonic solution and incubated for another 10 min to allow cleavage of the AM form. The normalized Ca^{2+} intensity was calculated using

$$\frac{\Delta F}{F_0}=\frac{F-F_0}{F_0},$$

where F and F_0 are the mean fluorescence intensities of individual cells at time t and t=0, respectively. Cell viability was measured using propidium iodide (2.5 µM, Thermo Fisher Scientific) after 2 h of shear flow. Propidium iodide was gently perfused into the channel and incubated for 15 min at 37°C.

Fluorescence imaging

Fluorescence images were obtained using an inverted microscope (Axiovert 200M, Zeiss) with a CCD camera (AxioCam, Zeiss). Nuclear size was imaged with a filter set [excitation (ex): 365/40; emission (em): 445/50 nm] and a 63× oil immersion objective. The Ca^{2+} images were obtained using a 20× objective with filter sets (ex: 470/40 nm; em: 525/50 nm) for MDCK wild type, and (ex: 550/25 nm; em: 605/70) for P1KD cells. Confocal images were obtained using a Zeiss LSM-510 microscope.

Immunocytochemistry

For immunocytochemistry, cells were fixed in 4% paraformaldehyde for 15 min, permeabilized with PBS containing 0.1% Triton X-100 (Sigma-Aldrich) for 15 min and blocked with 5% goat serum in PBS for 1 h at room temperature. Cells were incubated with the primary antibody, monoclonal mouse anti-lamin A (1:100, ab8980, Abcam) at 4°C overnight. This was followed by the secondary antibody, goat anti-mouse Alexa Fluor 488 (1:200 dilution in PBS; A-11001, Invitrogen) for 1 h at room temperature. Piezo1 was stained with rabbit polyclonal Piezo1 primary antibody (1:25; NBP1-78446, Novus Biologicals), followed by a goat anti-rabbit IgG secondary antibody (1:100; CY-1500-NB, Novus biologicals). F-actin was stained with phalloidin–Alexa Fluor 568 (1:100; A12380, Invitrogen) and incubated for 1 h at room temperature. After each step, the cells were washed with PBS. Before imaging, a 1:20 dilution of slow fade Gold Anti-fade Reagent (Invitrogen) was added to the cells to sustain the fluorescence.

Piezo1 knockdown

Oligonucleotides were designed according to the BLOCK-iT Pol II miR RNAi Expression Vector kit (Invitrogen) user manual and were as follows: DP1miRNA6864T, TGCTGTAAGGGTGACAGTAACATCGAGTTTTG-GCCACTGACTGACTCGATGTTTGTCACCCTTA; DP1miRNA6864B, CCTGTAAGGGTGACAAACATCGAGTCAGTCAGTGGCCAAAACT-CGATGTTACTGTCACCCTTAC. The oligonucleotides were annealed and then ligated with pcDNA 6.2-GW/EmGFP miR expression vector according to the BLOCK-iT Pol II miR RNAi Expression Vector protocol and transformed. DNA from single colonies was analyzed by sequencing.

To test for knockdown efficiency, MDCK-derived Piezo1 tagged with a mScarlet fluorescent protein (250 ng) and miRNA (750 ng) targeting Piezo1 were co-transfected into HEK293 cells. Total RNA was isolated from the cells after indicated times using Macherey-Nagel's NucleoSpin RNA Plus kit. Reverse transcription (RT)-PCR was performed on 250 ng total RNA using Invitrogen Superscript III First Strand Synthesis System. 3 µl of this reaction was then used in a qPCR reaction with primers for canine Piezo1 and β-actin, 5 µl of each reaction was then run on a 0.8% agarose gel (Fig. S3B,C). Band intensities were measured in ImageJ software.

Cell culture and transfection

Madin–Darby canine kidney (MDCK) cells (ATCC) were grown to confluence in Dulbecco's modified Eagle's medium (DMEM) containing 10% fetal bovine serum, 1% penicillin and streptomycin. The cell suspension was perfused into the microfluidic chamber and grown for ∼3 days to ∼90% confluence. The culture media was changed every 24 h. Isotonic saline solutions were used during imaging to reduce background fluorescence. To knock down Piezo1, cells were transfected with a plasmid encoding EGFP and miRNA targeting *Piezo1* mRNA (0.4 µg), using Effectene (Qiagen) according to the manufacturer's specification. Cells were cultured for an additional 48 h prior to experiments.

Solution and chemicals

Normal saline containing 1 mM $CaCl_2$ was used as a control solution. For Ca^{2+}-free solutions, $CaCl_2$ was replaced by $MgCl_2$. Yoda1 (Tocris Bioscience) was dissolved in DMSO as stock solution (48 mM), then diluted in saline to a final concentration of 25 µM. Gadolinium chloride, thapsigargin, ionophore A23187, and cytochalasin-D (all from Sigma-Aldrich) were prepared to final concentrations of 20 µM, 5 µM, 2 µM, and 10 µM, respectively.

Statistical analysis

For statistical analysis, the normalized nuclear areas or Ca^{2+} intensities were averaged over multiple cells in each image and across multiple experiments. A minimum of four experiments were performed for each condition. Fresh cells were used for each experiment. Data are shown as the mean±s.e.m. Statistical analysis used the paired sample *t*-test (confocal images used a two-sample *t*-test). Values of $P<0.005$ were considered statistically significant.

Acknowledgements

We thank Dr Wade J. Sigurdson at Confocal Microscope and Flow Cytometry Facility at University at Buffalo for help on confocal microcopy imaging, and Lynn Ziegler for Piezo1 miRNA cloning.

Competing interests

The authors declare no competing or financial interests.

Author contributions

Conceptualization: D.J., P.A.G., S.Z.H.; Methodology: D.J., P.A.G., S.Z.H.; Formal analysis: D.J., S.Z.H.; Investigation: D.J., S.Z.H.; Writing - original draft: S.Z.H.; Writing - review & editing: D.J., P.A.G., D.V., F.S., S.Z.H.; Supervision: P.A.G., S.Z.H.; Funding acquisition: F.S., S.Z.H.

Funding

This work was supported by National Science Foundation (CMMI-1537239).

Supplementary information

Supplementary information available online at
http://jcs.biologists.org/lookup/doi/10.1242/jcs.226076.supplemental

References

Aarts, M., Liu, Y., Liu, L., Besshoh, S., Arundine, M., Gurd, J. W., Wang, Y. T., Salter, M. W. and Tymianski, M. (2002). Treatment of ischemic brain damage by perturbing NMDA receptor- PSD-95 protein interactions. *Science* **298**, 846-850. doi:10.1126/science.1072873

Arnone, J. T., Walters, A. D. and Cohen-Fix, O. (2013). The dynamic nature of the nuclear envelope: lessons from closed mitosis. *Nucleus* **4**, 261-266. doi:10.4161/nucl.25341

Arsenovic, P. T., Ramachandran, I., Bathula, K., Zhu, R., Narang, J. D., Noll, N. A., Lemmon, C. A., Gundersen, G. G. and Conway, D. E. (2016). Nesprin-2G, a component of the nuclear LINC complex, is subject to myosin-dependent tension. *Biophys. J.* **110**, 34-43. doi:10.1016/j.bpj.2015.11.014

Bae, C., Sachs, F. and Gottlieb, P. A. (2011). The mechanosensitive ion channel piezo1 is inhibited by the peptide GsMTx4. *Biochemistry* **50**, 6295-6300. doi:10.1021/bi200770q

Balikov, D. A., Brady, S. K., Ko, U. H., Shin, J.-H., de Pereda, J. M., Sonnenberg, A., Sung, H. J. and Lang, M. J. (2017). The nesprin-cytoskeleton interface probed directly on single nuclei is a mechanically rich system. *Nucleus* **8**, 534-547. doi:10.1080/19491034.2017.1322237

Bray, M.-A. P., Adams, W. J., Geisse, N. A., Feinberg, A. W., Sheehy, S. P. and Parker, K. K. (2010). Nuclear morphology and deformation in engineered cardiac myocytes and tissues. *Biomaterials* **31**, 5143-5150. doi:10.1016/j.biomaterials.2010.03.028

Broers, J. L. V., Ramaekers, F. C. S., Bonne, G., Yaou, R. B. and Hutchison, C. J. (2006). Nuclear lamins: laminopathies and their role in premature ageing. *Physiol. Rev.* **86**, 967-1008. doi:10.1152/physrev.00047.2005

Carpenter, A. E., Jones, T. R., Lamprecht, M. R., Clarke, C., Kang, I. H., Friman, O., Guertin, D. A., Chang, J. H., Lindquist, R. A., Moffat, J. et al. (2006). CellProfiler: image analysis software for identifying and quantifying cell phenotypes. *Genome Biol.* **7**, R100. doi:10.1186/gb-2006-7-10-r100

Chambliss, A. B., Khatau, S. B., Erdenberger, N., Robinson, D. K., Hodzic, D., Longmore, G. D. and Wirtz, D. (2013). The LINC-anchored actin cap connects the extracellular milieu to the nucleus for ultrafast mechanotransduction. *Sci. Rep.* **3**, 1087. doi:10.1038/srep01087

Chan, C. J., Li, W., Cojoc, G. and Guck, J. (2017). Volume transitions of isolated cell nuclei induced by rapid temperature increase. *Biophys. J.* **112**, 1063-1076. doi:10.1016/j.bpj.2017.01.022

Chang, W., Worman, H. J. and Gundersen, G. G. (2015). Accessorizing and anchoring the LINC complex for multifunctionality. *J. Cell Biol.* **208**, 11-22. doi:10.1083/jcb.201409047

Coste, B., Mathur, J., Schmidt, M., Earley, T. J., Ranade, S., Petrus, M. J., Dubin, A. E. and Patapoutian, A. (2010). Piezo1 and Piezo2 are essential components of distinct mechanically activated cation channels. *Science* **330**, 55-60. doi:10.1126/science.1193270

Coste, B., Xiao, B., Santos, J. S., Syeda, R., Grandl, J., Spencer, K. S., Kim, S. E., Schmidt, M., Mathur, J., Dubin, A. E. et al. (2012). Piezo proteins are pore-forming subunits of mechanically activated channels. *Nature* **483**, 176-181. doi:10.1038/nature10812

Crisp, M. (2006). Coupling of the nucleus and cytoplasm: role of the LINC complex. *J. Cell Biol.* **172**, 41-53. doi:10.1083/jcb.200509124

Duan, Y., Gotoh, N., Yan, Q., Du, Z., Weinstein, A. M., Wang, T. and Weinbaum, S. (2008). Shear-induced reorganization of renal proximal tubule cell actin cytoskeleton and apical junctional complexes. *Proc. Natl. Acad. Sci. USA* **105**, 11418-11423. doi:10.1073/pnas.0804954105

Eddy, R. J., Pierini, L. M., Matsumura, F. and Maxfield, F. R. (2000). Ca^{2+}-dependent myosin II activation is required for uropod retraction during neutrophil migration. *J. Cell Sci.* **113**, 1287-1298.

Eisenhoffer, G. T., Loftus, P. D., Yoshigi, M., Otsuna, H., Chien, C.-B., Morcos, P. A. and Rosenblatt, J. (2012). Crowding induces live cell extrusion to maintain homeostatic cell numbers in epithelia. *Nature* **484**, 546-549. doi:10.1038/nature10999

Essig, M., Terzi, F., Burtin, M. and Friedlander, G. (2001). Mechanical strains induced by tubular flow affect the phenotype of proximal tubular cells. *Am. J. Physiol. Renal Physiol.* **281**, F751-762. doi:10.1152/ajprenal.2001.281.4.F751

Finan, J. D. and Guilak, F. (2010). The effects of osmotic stress on the structure and function of the cell nucleus. *J. Cell. Biochem.* **109**, 460-467. doi:10.1002/jcb.22437

Grevesse, T., Versaevel, M., Circelli, G., Desprez, S. and Gabriele, S. (2013). A simple route to functionalize polyacrylamide hydrogels for the independent tuning of mechanotransduction cues. *Lab. Chip* **13**, 777-780. doi:10.1039/c2lc41168g

Gudipaty, S. A., Lindblom, J., Loftus, P. D., Redd, M. J., Edes, K., Davey, C. F., Krishnegowda, V. and Rosenblatt, J. (2017). Mechanical stretch triggers rapid epithelial cell division through Piezo1. *Nature* **543**, 118-121. doi:10.1038/nature21407

Gupta, S., Marcel, N., Sarin, A. and Shivashankar, G. V. (2012). Role of actin dependent nuclear deformation in regulating early gene expression. *PLoS ONE* **7**, e53031. doi:10.1371/journal.pone.0053031

Hale, C. M., Shrestha, A. L., Khatau, S. B., Stewart-Hutchinson, P. J., Hernandez, L., Stewart, C. L., Hodzic, D. and Wirtz, D. (2008). Dysfunctional connections between the nucleus and the actin and microtubule networks in laminopathic models. *Biophys. J.* **95**, 5462-5475. doi:10.1529/biophysj.108.139428

He, L., Si, G., Huang, J., Samuel, A. D. T. and Perrimon, N. (2018). Mechanical regulation of stem-cell differentiation by the stretch-activated Piezo channel. *Nature* **555**, 103-106. doi:10.1038/nature25744

Hua, S. Z., Gottlieb, P. A., Heo, J. and Sachs, F. (2010). A mechanosensitive ion channel regulating cell volume. *Am. J. Physiol. Cell Physiol.* **298**, C1424-C1430. doi:10.1152/ajpcell.00503.2009

Ihalainen, T. O., Aires, L., Herzog, F. A., Schwartlander, R., Moeller, J. and Vogel, V. (2015). Differential basal-to-apical accessibility of lamin A/C epitopes in the nuclear lamina regulated by changes in cytoskeletal tension. *Nat. Mater.* **14**, 1252-1261. doi:10.1038/nmat4389

Isermann, P. and Lammerding, J. (2013). Nuclear mechanics and mechanotransduction in health and disease. *Curr. Biol.* **23**, R1113-R1121. doi:10.1016/j.cub.2013.11.009

Karaki, H., Ozaki, H., Hori, M., Mitsui-Saito, M., Amano, K., Harada, K., Miyamoto, S., Nakazawa, H., Won, K. J. and Sato, K. (1997). Calcium movements, distribution, and functions in smooth muscle. *Pharmacol. Rev.* **49**, 157-230.

Lammerding, J., Hsiao, J., Schulze, P. C., Kozlov, S., Stewart, C. L. and Lee, R. T. (2005). Abnormal nuclear shape and impaired mechanotransduction in emerin-deficient cells. *J. Cell Biol.* **170**, 781-791. doi:10.1083/jcb.200502148

Li, J., Hou, B., Tumova, S., Muraki, K., Bruns, A., Ludlow, M. J., Sedo, A., Hyman, A. J., McKeown, L., Young, R. S. et al. (2014a). Piezo1 integration of vascular architecture with physiological force. *Nature* **515**, 279-282. doi:10.1038/nature13701

Li, Q., Kumar, A., Makhija, E. and Shivashankar, G. V. (2014b). The regulation of dynamic mechanical coupling between actin cytoskeleton and nucleus by matrix geometry. *Biomaterials* **35**, 961-969. doi:10.1016/j.biomaterials.2013.10.037

Lombardi, M. L., Jaalouk, D. E., Shanahan, C. M., Burke, B., Roux, K. J. and Lammerding, J. (2011). The interaction between nesprins and sun proteins at the nuclear envelope is critical for force transmission between the nucleus and cytoskeleton. *J. Biol. Chem.* **286**, 26743-26753. doi:10.1074/jbc.M111.233700

Lovett, D. B., Shekhar, N., Nickerson, J. A., Roux, K. J. and Lele, T. P. (2013). Modulation of nuclear shape by substrate rigidity. *Cell. Mol. Bioeng.* **6**, 230-238. doi:10.1007/s12195-013-0270-2

Lu, W., Schneider, M., Neumann, S., Jaeger, V.-M., Taranum, S., Munck, M., Cartwright, S., Richardson, C., Carthew, J., Noh, K. et al. (2012). Nesprin interchain associations control nuclear size. *Cell. Mol. Life Sci.* **69**, 3493-3509. doi:10.1007/s00018-012-1034-1

Maneshi, M. M., Ziegler, L., Sachs, F., Hua, S. Z. and Gottlieb, P. A. (2018). Enantiomeric Aβ peptides inhibit the fluid shear stress response of PIEZO1. *Sci. Rep.* **8**, 14267. doi:10.1038/s41598-018-32572-2

McHugh, B. J., Buttery, R., Lad, Y., Banks, S., Haslett, C. and Sethi, T. (2010). Integrin activation by Fam38A uses a novel mechanism of R-Ras targeting to the endoplasmic reticulum. *J. Cell Sci.* **123**, 51-61. doi:10.1242/jcs.056424

Neelam, S., Hayes, P. R., Zhang, Q., Dickinson, R. B. and Lele, T. P. (2016). Vertical uniformity of cells and nuclei in epithelial monolayers. *Sci. Rep.* **6**, 19689. doi:10.1038/srep19689

Nourse, J. L. and Pathak, M. M. (2017). How cells channel their stress: interplay between Piezo1 and the cytoskeleton. *Semin. Cell Dev. Biol.* **71**, 3-12. doi:10.1016/j.semcdb.2017.06.018

Pathak, M. M., Nourse, J. L., Tran, T., Hwe, J., Arulmoli, J., Le, D. T. T., Bernardis, E., Flanagan, L. A. and Tombola, F. (2014). Stretch-activated ion channel Piezo1 directs lineage choice in human neural stem cells. *Proc. Natl. Acad. Sci. USA* **111**, 16148-16153. doi:10.1073/pnas.1409802111

Pennell, T., Suchyna, T., Wang, J., Heo, J., Felske, J. D., Sachs, F. and Hua, S. Z. (2008). Microfluidic chip to produce temperature jumps for electrophysiology. *Anal. Chem.* **80**, 2447-2451. doi:10.1021/ac702169t

Philip, J. T. and Dahl, K. N. (2008). Nuclear mechanotransduction: response of the lamina to extracellular stress with implications in aging. *J. Biomech.* **41**, 3164-3170. doi:10.1016/j.jbiomech.2008.08.024

Rahimzadeh, J., Meng, F., Sachs, F., Wang, J., Verma, D. and Hua, S. Z. (2011). Real-time observation of flow-induced cytoskeletal stress in living cells. *Am. J. Physiol. Cell Physiol.* **301**, C646-C652. doi:10.1152/ajpcell.00099.2011

Ranade, S. S., Qiu, Z., Woo, S.-H., Hur, S. S., Murthy, S. E., Cahalan, S. M., Xu, J., Mathur, J., Bandell, M., Coste, B. et al. (2014). Piezo1, a mechanically activated ion channel, is required for vascular development in mice. *Proc. Natl. Acad. Sci. USA* **111**, 10347-10352. doi:10.1073/pnas.1409233111

Stuurman, N., Heins, S. and Aebi, U. (1998). Nuclear lamins: their structure, assembly, and interactions. *J. Struct. Biol.* **122**, 42-66. doi:10.1006/jsbi.1998.3987

Syeda, R., Xu, J., Dubin, A. E., Coste, B., Mathur, J., Huynh, T., Matzen, J., Lao, J., Tully, D. C., Engels, I. H. et al. (2015). Chemical activation of the mechanotransduction channel Piezo1. *eLife* **4**, e07369. doi:10.7554/eLife.07369

Uzer, G., Thompson, W. R., Sen, B., Xie, Z., Yen, S. S., Miller, S., Bas, G., Styner, M., Rubin, C. T., Judex, S. et al. (2015). Cell mechanosensitivity to extremely low-magnitude signals is enabled by a LINCed nucleus. *Stem Cells* **33**, 2063-2076. doi:10.1002/stem.2004

Verma, D., Ye, N., Meng, F., Sachs, F., Rahimzadeh, J. and Hua, S. Z. (2012). Interplay between cytoskeletal stresses and cell adaptation under chronic flow. *PLoS ONE* **7**, e44167. doi:10.1371/journal.pone.0044167

Versaevel, M., Grevesse, T. and Gabriele, S. (2012). Spatial coordination between cell and nuclear shape within micropatterned endothelial cells. *Nat. Commun.* **3**, 671. doi:10.1038/ncomms1668

Versaevel, M., Braquenier, J.-B., Riaz, M., Grevesse, T., Lantoine, J. and Gabriele, S. (2014). Super-resolution microscopy reveals LINC complex recruitment at nuclear indentation sites. *Sci. Rep.* **4**, 7362. doi:10.1038/srep07362

Wang, N., Tytell, J. D. and Ingber, D. E. (2009). Mechanotransduction at a distance: mechanically coupling the extracellular matrix with the nucleus. *Nat. Rev. Mol. Cell Biol.* **10**, 75-82. doi:10.1038/nrm2594

Zhou, J. (2009). Polycystins and primary cilia: primers for cell cycle progression. *Annu. Rev. Physiol.* **71**, 83-113. doi:10.1146/annurev.physiol.70.113006.100621

Zhu, Q., Zheng, F., Liu, A. P., Qian, J., Fu, C. and Lin, Y. (2016). Shape transformation of the nuclear envelope during closed mitosis. *Biophys. J.* **111**, 2309-2316. doi:10.1016/j.bpj.2016.10.004